Synthesis and characterization of nanocrystalline $Al_{0.5}Ag_{0.5}TiO_3$ powder

Sandeep Kumar[1], L.K. Sahay[1], Anal K. Jha[2] and K. Prasad[*2,3]

[1]*University Department of Chemistry, T.M. Bhagalpur University, Bhagalpur 812 007, India*
[2]*Aryabhatta Centre for Nanoscience and Nanotechnology, Aryabhatta Knowledge University, Patna 800 001, India*
[3]*University Department of Physics, T.M. Bhagalpur University, Bhagalpur 812 007, India*

Abstract. A low-cost, green and reproducible citric acid assisted synthesis of nanocrystalline $Al_{0.5}Ag_{0.5}TiO_3$ (n-AAT) powder is reported. X-ray, FTIR, energy dispersive X-ray, transmission electron microscopy and scanning electron microscopy analyses are performed to ascertain the formation of n-AAT. X-ray diffraction data analysis indicated the formation of monoclinic structure. Spherical shaped particles having the sizes of 3-15 nm are found. The mechanism of nano-transformation for the soft-chemical synthesis of n-AAT has been explained using simple organic chemistry rules and nucleation and growth theory. Dielectric study revealed that AAT ceramic might be a suitable candidate for capacitor applications.

Keywords: green synthesis; citric acid gel method; nanoparticle; dielectric properties; $Al_{0.5}Ag_{0.5}TiO_3$

1. Introduction

Perovskite ABO_3–type lead containing materials, such as $Pb(Zr,Ti)O_3$, $Pb(Mg_{1/3}Nb_{2/3})O_3$–$PbTiO_3$ and $Pb(Zn_{1/3}Nb_{2/3})O_3$–$PbTiO_3$ in ceramic or crystal form, are being used for different electronic and/or microelectronic devices (Eichel and Kungl 2010, Rödel *et al.* 2009). However, the toxicity of lead oxide and its high vapor pressure during sintering processing cause serious environmental problems. It is, therefore, necessary to develop alternative lead-free materials that should be ecofriendly from the viewpoint of sustainable development (Fancher *et al.* 2013, Prasad *et al.* 2013, Kumari *et al.* 2011, Damjanovic *et al.* 2010, Shrout and Zhang 2007, Takenaka and Nagata 2005, Cross 2004). Among them bismuth sodium titanate, $Bi_{0.5}Na_{0.5}TiO_3$, discovered by Smolenskii, in 1960, is considered to be an excellent candidate as a key lead-free material, which shows strong ferroelectric properties (Hiruma *et al.* 2009, Prasad *et al.* 2007, Smolenskii *et al.* 1961). Recent works on the identical silver-based compounds such as $Bi_{0.5}Ag_{0.5}TiO_3$ (Inaguma *et al.* 2001, Park *et al.* 1999), $Bi_{0.5}(Na_{1-x-y}K_xAg_y)_{0.5}TiO_3$ (Liao *et al.* 2008), $Fe_{0.5}Ag_{0.5}TiO_3$ (Kumar *et al.* 2013), $NaNbO_3$-$Bi_{0.5}A_{0.5}TiO_3$ (A = Li, Na, K, Ag) (Raevskii *et al.* 2000), $Bi_{0.5}Na_{0.5}TiO_3$-$BaTiO_3$-$Bi_{0.5}Ag_{0.5}TiO_3$ (Wu *et al.* 2011), $Bi_{0.5}Na_{0.5}TiO_3$-$Bi_{0.5}K_{0.5}TiO_3$-$Bi_{0.5}Ag_{0.5}TiO_3$ (Lu *et al.* 2007, Lu *et al.* 2008), also showed excellent electrical properties. Further search of new lead-free

---

∗Corresponding author, Ph.D., E-mail: k.prasad65@gmail.com; k_prasad65@yahoo.co.in

alternative, one such material in this series is perovskite $Al_{0.5}Ag_{0.5}TiO_3$. The material is environment-friendly, mechanically tough and displayed very low loss $\sim 10^{-2}$ which indicates that this compound is having the potential for capacitor applications. Besides, extensive literature survey indicated that no attempt, to the authors' knowledge, has so far been made to study nanocrystalline $Al_{0.5}Ag_{0.5}TiO_3$ (abbreviated hereafter as n-AAT) powder. Accordingly, present work reports the synthesis (using citric acid gel method) of n-AAT and their structural (X-ray and its Rietveld analysis), transmission electron microscopy, scanning electron microscopy and Fourier transformed infrared spectroscopy studies. The dielectric properties have also been carried out to see its potential for capacitor applications. Besides, the mechanism of nanotransformation for the soft-chemical synthesis of n-AAT has been explained using simple organic chemistry rules and nucleation and growth theory.

2. Experimental details

2.1 Synthesis of nanocrystalline $Al_{0.5}Ag_{0.5}TiO_3$ powder

A citric acid gel method was used to prepare $Al_{0.5}Ag_{0.5}TiO_3$ powder. Citric acid was dissolved into deionized water and the value of the pH of the solution was adjusted to 7–8 by adding the appropriate amount of ammonia solution. Titanium (IV) n-Butoxide (Across, USA) was added to this solution which was vigorously stirred and heated at about 70°C for 1 h on a hot plate. This solution was then added with aqueous solutions of $AgNO_3$ (Merck, Germany) and $Al(NO_3)_3.9H_2O$ (Across, USA) and stirred at 80°C for 2 h. Further, the precursor solution was dehydrated at 100°C to form a sol. Subsequent heating at a higher temperature of 160°C yield a gel. The gel initially tends to swell and filled the beaker producing a foamy precursor. The gel was pulverized and then heated at 300°C for 2 h in air to get carbonaceous mass. Finally carbonaceous mass was calcined at 700°C for 5 h. Completion of the reaction and formation of the desired compound was checked by X-ray diffraction technique. The as-calcined powder was compacted into thin (~ 1.5 mm) cylindrical disks with an applied uniaxial pressure of 650 MPa. These pellets were then sintered in air atmosphere at 750°C for 3 h in alumina crucible.

2.2 Characterization

X-ray diffraction (XRD) data of n-AAT were obtained using an X-ray diffractometer (XPERT-PRO, PW3050/60) with CuK_α radiation ($\lambda = 1.5406$Å) between the angles 20° and 80°. TEM micrographs and selected area diffraction (SAED) and energy dispersive X-ray (EDX) patterns of n-AAT were obtained using High resolution Bruker transmission electron microscope. SEM micrograph of n-AAT was taken using a computer controlled scanning electron microscope (JEOL-JSM840A). The Fourier Transformed Infrared (FTIR) spectrum of n-AAT was collected in the transmission mode using an Alpha-T Bruker FTIR spectrophotometer in the range of 400-4000 cm^{-1}. A sintered pellet was polished and electroded with air-drying silver paste (SPI supplier, USA) to measure the electrical properties. Dielectric measurement was carried out using a computer-interfaced LCR Hi-Tester (HIOKI 3532-50, Japan) in a cooling mode to avoid the moisture, if any. Further, the temperature coefficient of capacitance (T_{CC}) which is an important parameter for the low-temperature dependence of capacitance is defined as: $T_{cc}(\%) = [(C_T - C_{RT})/C_{RT}] \times 100$; where C_T and C_{RT} represent the values of capacitance at the elevated

and at room temperature, respectively.

3. Results and discussion

Rietveld refinement of the XRD data of n-AAT was carried out, selecting the space group $P2/m(10)$. The XRD (observed, calculated and difference XRD profiles) pattern of n-AAT synthesized using citric acid gel method is presented in Fig. 1. It can be seen that the profiles for observed and calculated one are perfectly matching ($\chi^2 = 1.28$). The profile fitting procedure adopted was minimizing the χ^2 function (McCusker *et al.* 1999). The XRD analyses indicated that n-AAT has a monoclinic unit cell. The crystal data and refinement factors of n-AAT obtained from XRD data are depicted in Table 1. Further, the XRD patterns showed the presence of broad peaks which may be due the nanosizing effect in n-AAT.

Fig. 2 shows the EDX pattern and TEM image (inset) of n-AAT. All the peaks in the EDX pattern have perfectly assigned to the elements present in $Al_{0.5}Ag_{0.5}TiO_3$. This clearly indicated the successful synthesis and purity of chemical composition of n-AAT. The HR-TEM micrograph (inset Fig. 2) clearly illustrates individual nanoparticles which are almost spherical in shape. This observation has also been supported by the SEM micrograph (Fig. 3(ii)) which clearly ensures the formation of spherical nanoparticles of AAT. The particle size distribution histogram of n-AAT is shown in the inset of Fig. 3(i)(a), which shows that the particles having the sizes between 3-15 nm are present in TEM micrograph (Fig. 3(i)). The difference in size may possibly be due to the agglomeration of individual nanoparticles and are being formed at different times. Inset Fig. 3(i)(b) illustrates Scherrer rings in the SAED pattern which clearly indicates the formation nanocrystalline AAT particles. Indexing of SAED pattern revealed the monoclinic lattice structure, which is in agreement with XRD result.

The FTIR spectrum (Fig. 4) exhibits a prominent fundamental absorption band at 525 cm⁻¹, which is due to Ti–O vibration. Multiple peaks (A-O absorption bands) in the frequency region
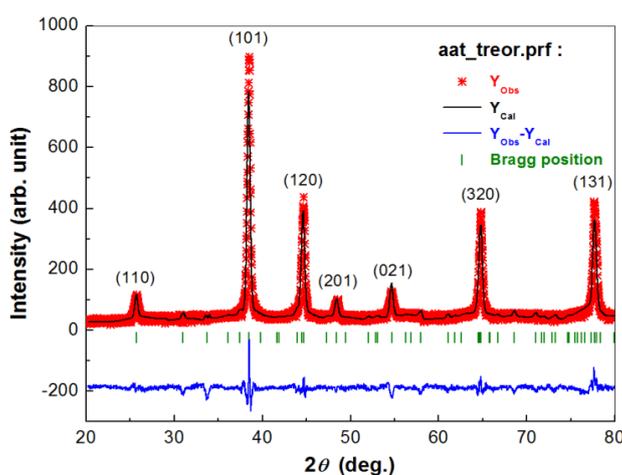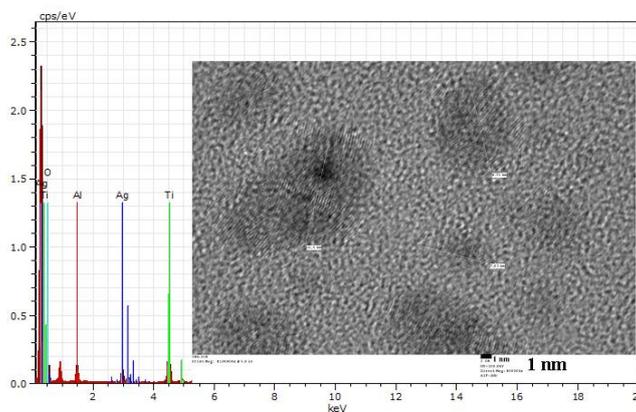

Fig. 1 Rietveld refined XRD pattern of nanocrystalline powder of $Al_{0.5}Ag_{0.5}TiO_3$ in the space group $P2/m(10)$. Symbols represent observed data points and solid lines their Rietveld fit

Table 1 The crystal data and refinement factors of $Al_{0.5}Ag_{0.5}TiO_3$ obtained from X-ray powder diffraction data

Crystallographic data		Description of parameters:
Formula	$Al_{0.5}Ag_{0.5}TiO_3$	
Crystal System	Monoclinic	R_p (profile factor) = $100[\Sigma|y_i-y_{ic}|/\Sigma|y_i|]$, where y_i is
Space group (No.)	$P2/m$ (10)	the observed intensity and y_{ic} is the calculated
a (Å)	5.7819	intensity at the ith step.
b (Å)	4.3314	
c (Å)	2.6611	R_{wp} (weighted profile factor) = $100[\Sigma\omega_i|y_i-$
β (°)	94.6087	$y_{ic}|^2/\Sigma\omega_i(y_i)^2]^{1/2}$, where $\omega_i=1/\sigma_i^2$ and σ_i^2 is variance
V (Å^3)	66.4256	of the observation.
Data collection		
Temperature (°C)	24.0	R_{exp} (expected weighted profile factor) = $100[(n-$
Wavelength [CuK$_\alpha$] (Å)	1.5406	$p)/\Sigma\omega_i(y_i)^2]^{1/2}$, where n and p are the number of
Monochromator	Graphite	profile points and refined parameters, respectively.
Measuring range (°)	$20 \le 2\theta \le 80$	
Step (°2θ)	0.02	R_B (Bragg factor) = $100[\Sigma|I_{obs}-I_{calc}|/\Sigma|I_{obs}|]$, where
Integration time (s)	30	I_{obs} is the observed integrated intensity and I_{calc} is the calculated integrated intensity.
Rietveld data		
Program	FULLPROF	R_F (crystallographic R_F factor) = $100[\Sigma|F_{obs}-$
Function for background level	Polynomial 5-order	$F_{calc}|/\Sigma|F_{obs}|]$, where F is the structure factor, $F =$
Function for peak shape	Pseudo-Voigt	$\sqrt{(I/L)}$, where L is Lorentz polarization factor.
R_p	35.4	
R_{wp}	31.1	$\chi^2 = \Sigma\omega_i(y_i-y_{ic})^2$.
R_{exp}	27.5	
R_B	0.179	d (Durbin–Watson statistics) = $\Sigma\{[\omega_i(y_i-y_{ic})-\omega_{i-1}(y_{i-1}-$
R_F	0.395	$y_{ic-1})]^2\}/\Sigma[\omega_i(y_i-y_{ic})]^2$.
χ^2	1.28	
d	0.7402	Q_D = expected d.
Q_D	1.8996	
S	1.1309	S (goodness of fit) = (R_{wp}/R_{exp}).

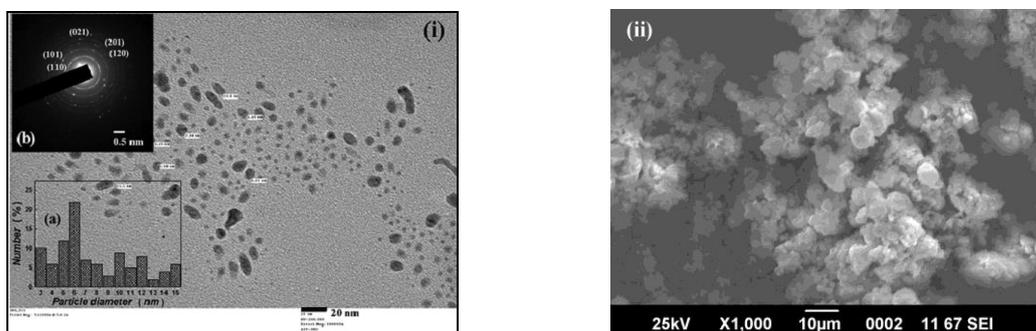Fig. 2 EDX spectrum and HR-TEM image (inset) of nanocrystalline $Al_{0.5}Ag_{0.5}TiO_3$ powder

Fig. 3 (i) TEM image, particle size distribution (inset: a), SAED pattern (inset: b) and (ii) SEM image of nanocrystalline Al$_{0.5}$Ag$_{0.5}$TiO$_3$ powder
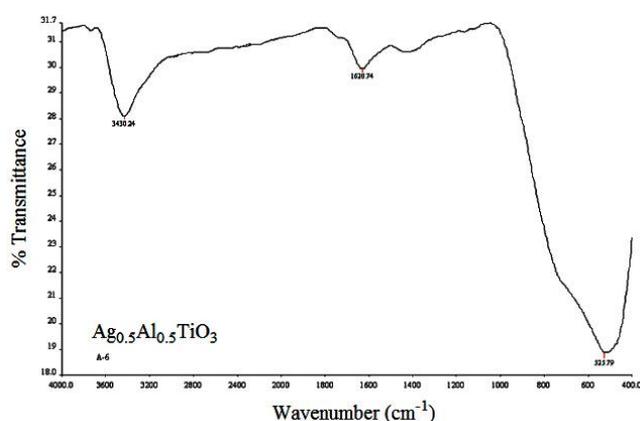

Fig. 4 FTIR spectrum of nanocrystalline Al$_{0.5}$Ag$_{0.5}$TiO$_3$ powder

900-1630 cm^{-1} are due to the presence of Al-O and Ag-O vibrations (Kumar *et al.* 2013). Further, a broad and strong peak can easily be seen at 3430 cm^{-1} which is due to free water molecules (H$_2$O bands) and strong stretching (antisymmetric and symmetric) modes of the OH group. No other band appeared in the FTIR spectrum clearly revealed the formation of Al$_{0.5}$Ag$_{0.5}$TiO$_3$ calcination at 700°C.

The schematic for the soft chemical synthesis of n-AAT is illustrated in Fig. 5. Citric acid and citrate ions are readily inter-convertible requiring and/or releasing an appreciable amount of free energy ($\Delta G \sim 47$ KJ/mol) in aqueous medium (Miller and Magowan 1990, Jha *et al.* 2011) which is probably sufficient enough to accomplish nano-transformation. Present nano-transformation mechanism could be understood using the nucleation and growth theory to form a spherical particle. According to which the overall free energy change must be overcome. ΔG is the indicative of sum of the free energy due to the formation of a new volume and the free energy due to the new surface created: $\Delta G = -\frac{4}{V} \pi r^3 k_B T \ln(S) + 4\pi r^2 \gamma$, where V, r, k_B, S and γ are the molecular volume of the prepared species, radius of the nucleus, Boltzmann constant, saturation ratio and surface free energy per unit surface area, respectively. It follows from equation that a decrease in γ or an increase in S is helpful in the formation of nanoparticles (n-AAT, in this case). Besides, R-COOH makes a non-equivalent resonating structure whereas RCOO$^-$ efficiently makes
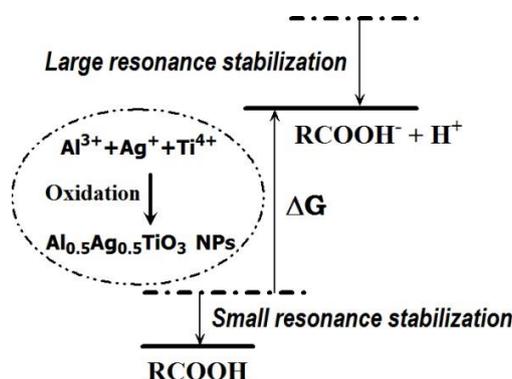
Fig. 5 Schematic for the synthesis of nanocrystalline $Al_{0.5}Ag_{0.5}TiO_3$ powder using citric acid gel method
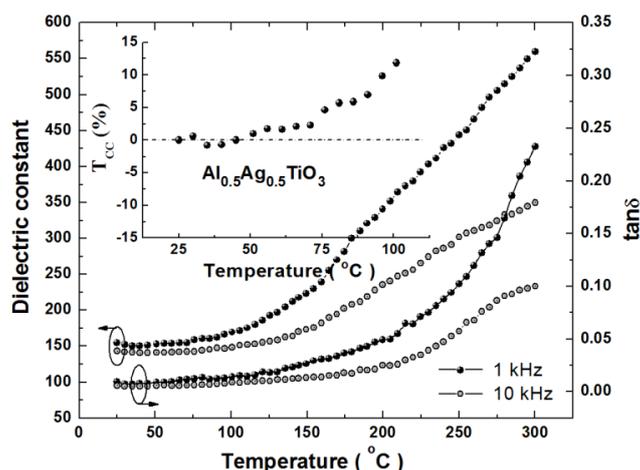

Fig. 6 Temperature dependence of dielectric constant and loss tangent of $Al_{0.5}Ag_{0.5}TiO_3$ ceramic pellet at 1 kHz and 10 kHz. Inset: Variation of T_{CC}(%) with temperature at 1 kHz

an equivalent one. This way, the resonance energy of stabilization of R-COOH is larger than that of $RCOO^-$ and this energy of dissociation probably remains available all along in the incubation medium for nano-transformation of both metal as well as oxide system, as the case may be (Morrison and Boyd 1983, Jha *et al.* 2011). In the present soft-chemical method, the interactions of citric acid with Al^{3+}, Ag^+ and Ti^{4+} ions in stoichiometric ratio made it possible to lower down the surface energy. Therefore, the effect of such soft-chemical ambiance could have made the reaction to occur more easily.

Fig. 6 shows the variation of dielectric constant (ε) and loss tangent (tanδ) with temperature at 1 kHz and 10 kHz. It is observed that values of both ε and tanδ increase with increment in temperature in the investigated temperature range. The room temperature values of ε and tanδ are, respectively, found to be 155 and 0.0092 at 1 kHz. Since the observation was made for only in a limited range of temperature dielectric anomaly could not be observed as similar material *e.g.* $(Ag_{0.5}Bi_{0.5})TiO_3$ has very high phase transition temperature (~800 K) (Inaguma *et al.* 2001). It can

also be noted that the value of tanδ are of the order of 10^{-2} in the working temperature range (up to 100°C). The low tanδ of this kind can be advantageous when improved detectivity (pyroelectric applications) is required. Inset of Fig. 5 clearly illustrates that the values of T_{CC} varies within $\pm$ 12% in the working temperature range (upto +100°C). Therefore, the low value of T_{CC} ($< \pm12\%$), ε' (=155) and low tanδ ($\sim10^{-2}$) were found in case of n-AAT ceramic, which meets the specifications for "Z7R" of Class I dielectrics of Electronic Industries Association. Therefore, this compound may be considered as a potential candidate for capacitor applications.

4. Conclusions

In summary, the present soft-chemical method is truly a green cost-effective approach, capable of producing nanocrystalline Al$_{0.5}$Ag$_{0.5}$TiO$_3$ powder. Nanocrystalline AAT powder was found to have a perovskite-type monoclinic structure with the particle sizes of 3-15 nm. EDX and FTIR studies confirmed the formation of pure AAT. A decrease in surface free energy per unit surface area or an increase in saturation ratio is helpful in the formation of AAT nanoparticles. Dielectric study revealed that this compound is having low dielectric constant (= 155), loss tangent (= 0.0092) at 1 kHz and a low T_{CC} ($< \pm12\%$) in the working temperature range (upto +100°C) which makes this material suitable for capacitor application and may be designated as 'Z7R' Class I material as per the specifications of the Electronic Industries Association.

Acknowledgements

References

Cross, L.E. (2004), "Lead-free at last", *Nature*, **432**, 24-25.
Damjanovic, D., Klein, N., Li, J. and Porokhonskyy, V. (2010), "What can be expected from lead-free piezoelectric materials?", *Funct. Mater. Lett.*, **3**, 5-13.
Eichel, R.A. and Kungl, H. (2010), "Recent developments and future perspectives of lead-free ferroelectrics", *Funct. Mater. Lett.*, **3**, 1-4.
Fancher, C.M., Blendell J. E. and Bowman, K.J. (2013), "Poling effect on d_{33} in textured Bi$_{0.5}$Na$_{0.5}$TiO$_3$-based materials", *Scripta Materialia*, **68**, 443-446.
Hiruma, Y., Nagata, H. and Takenaka, T. (2009), "Thermal depoling process and piezoelectric properties of bismuth sodium titanate ceramics", *J. Appl. Phys.*, **105**, 084112-084120.
Inaguma, Y., Katsumata, T., Wang, R., Kobashi, K., Itoh, M., Shan, Y.-J. and Nakamura, T. (2001), "Synthesis and dielectric properties of a perovskite Bi$_{1/2}$Ag$_{1/2}$TiO$_3$", *Ferroelectr.*, **264**, 127-132.
Jha, A.K., Kumar, V. and Prasad, K. (2011), "Biosynthesis of metal and oxide nanoparticles using orange juice", *J. Bionanosci.*, **5**, 162-165.
Kumar, S., Sahay, L.K., Jha, A.K. and Prasad, K. (2013), "Synthesis of (Ag$_{0.5}$Fe$_{0.5}$)TiO$_3$ nanocrystalline powders using stearic acid gel method", *Adv. Mater. Lett.*, DOI: 10.5185/amlett.2013.fdm.06.
Kumari, K., Prasad, A. and Prasad, K. (2011), "Structural and dielectric properties of ZnO added

$(Na_{1/2}Bi_{1/2})TiO_3$ ceramic", *J. Mater. Sci. Technol.*, **27**, 213-217.

Liao, Y., Xiao, D. and Lin, D. (2008), "Piezoelectric and ferroelectric properties of $Bi_{0.5}(Na_{1-x-y}K_xAg_y)_{0.5}TiO_3$ lead-free piezoelectric ceramics", *Appl. Phys. A: Mater. Sci. Process,* **90**, 165-169.

Lu, Y., Li, Y., Wang, D. and Yin, Q. (2007), "Morphotropic phase boundary and electrical properties of $(Bi_{1/2}Na_{1/2})TiO_3$-$(Bi_{1/2}K_{1/2})TiO_3$-$(Bi_{1/2}Ag_{1/2})TiO_3$ ceramics", *Ferroelectr.*, **358**, 109-116.

Lu, Y., Li, Y., Wang, D., Wang T. and Yin, Q. (2008), "Lead-free piezoelectric ceramics of $(Bi_{1/2}Na_{1/2})TiO_3$–$(Bi_{1/2}K_{1/2})TiO_3$–$(Bi_{1/2}Ag_{1/2})TiO_3$ system", *J. Electroceram.*, **21**, 309-313.

McCusker, L.B., Von Dreele, R.B., Cox, D.E., Louër, D. and Scardi, P. (1999), "Rietveld refinement guidelines", *J. Appl. Cryst.*, **32**, 36-50.

Miller, S. L. and Magowan, D. S. (1990), "The thermodynamics of the Krebs cycle and related compounds", *J. Phys. Chem. Re. Data*, **19**, 1049-1070.

Morrison, R.T. and Boyd, R.N. (1983), *Advanced Organic Chemistry*, Allyn and Bacon Inc., Boston, USA.

Park, J.H., Woodward, P.M., Parise, J.B., Reeder, R.J., Lubomirsky, I. and Stafsudd, O. (1999), "Synthesis, structure, and dielectric properties of $(Bi_{1/2}Ag_{1/2})TiO_3$", *Chem. Mater.*, **11**, 177-183.

Prasad, A., Roy, A.K. and Prasad, K. (2013), "Electrical conduction in $(Na_{0.5}Bi_{0.5})_{1-x}Ba_xTiO_3$ $(0 \leq x \leq 1)$ ceramic by complex impedance/modulus spectroscopy", *ISRN Ceram",* **2013**, Article ID 369670, 12 pages.

Prasad, K., Kumari, K., Lily, Chandra, K.P., Yadav, K.L. and Sen, S. (2007), "Electrical conduction in $(Na_{0.5}Bi_{0.5})TiO_3$ ceramic: Impedance spectroscopy analysis", *Adv. Appl. Ceram.*, **106**, 241-246.

Raevskii, I.P., Reznichenko, L.A. and Malitskaya, M.A. (2000), "Features in the dielectric properties and temperature-composition phase diagrams of $NaNbO_3$-$A_{0.5}Bi_{0.5}TiO_3$ (A = Li, Na, K, Ag) solid solutions", *Tech. Phys. Lett.*, **26**, 93-95.

Rödel, J., Jo, W., Seifert, K.T.P., Anton, E.M., Granzow, T. and Damjanovic, D. (2009), "Perspective on the Development of Lead-free Piezoceramics", *J. Am. Ceram. Soc.*, **92**, 1153-1177.

Shrout, T.R. and Zhang, S.J. (2007), "Lead-free piezoelectric ceramics: alternatives for PZT?", *J. Electroceram.*, **19**, 111-124.

Smolenskii, G.A., Isupov, V.A., Agranovskaya, A.I. and Krainik, N.N. (1961), "New ferroelectrics of complex composition IV", *Sov. Phys. Solid State*, **2**, 2651-2654.

Takenaka, T. and Nagata, H. (2005), "Current status and prospects of lead-free piezoelectric ceramics", *J. Euro. Ceram. Soc.*, **25**, 2693-2700.

Wu, L., Xiao, D., Zhou, F., Teng, Y. and Li, Y. (2011), "Microstructure, ferroelectric, and piezoelectric properties of $(1-x-y)Bi_{0.5}Na_{0.5}TiO_3-xBaTiO_3-yBi_{0.5}Ag_{0.5}TiO_3$ lead-free ceramics", *J. Alloys Comp.*, **509**, 466-470.

YH